Electromagnetic Induction Spectroscopy

I.J. Won and Dean Keiswetter

Geophex, Ltd. 605 Mercury Street, Raleigh, NC 27603

ABSTRACT

An object, made partly or wholly of metals, has a distinct combination of electrical conductivity, magnetic permeability, and geometrical shape and size. When the object is exposed to a low-frequency electromagnetic field, it produces a secondary magnetic field. By measuring the secondary field in a broadband spectrum, we obtain a distinct spectral signature that may uniquely identify the object. Based on the response spectrum, we attempt to "fingerprint" the object. This is the basic concept of *Electromagnetic Induction Spectroscopy (EMIS).*

EMIS technology may be particularly useful for detecting buried landmines and unexploded ordnance. By fully characterizing and identifying an object without excavation, we should be able to reduce significantly the number of false targets. EMIS should be fully applicable to many other problems where target identification and recognition (without intrusive search) are important. For instance, an advanced EMIS device at an airport security gate may be able to recognize a particular weapon by its maker and type.

Keywords: electromagnetic induction spectroscopy, discrimination, landmines, unexploded ordnance, geophysical sensor

STATEMENT OF PROBLEM

Geophysical sensors for detecting landmines and unexploded ordnance (UXO) include mainly magnetometers and EMI-based metal detectors. A magnetometer can detect only ferrous objects. Metal detectors can detect both ferrous and nonferrous targets, thus, they are more useful as stand-alone sensors than as magnetometers. Despite popular interest and enthusiasm, ground-probing radar (GPR) is yet to demonstrate its usefulness as a stand-alone sensor.

Conventional metal detectors are not designed to do any more than simply detect the presence of buried metal objects, because most of them operate at a factory-set single frequency. A few detectors may have capability of operating at two or so discrete frequencies. These detectors have no ability to discriminate ordnance from trash metals and, therefore, the false alarm rate is unacceptably high. We believe that the EMIS technology can provide both detection and discrimination capabilities.

INTRODUCTION

When an electrically conductive and/or magnetically permeable object is placed in a time-varying electromagnetic field, a system of induced current flows through the object. By observing a small secondary magnetic field emanating from the induced current, we attempt to detect the object; this is the foundation of the time-honored electromagnetic induction (EMI) method. EMI physics is completely described by Maxwell's four equations, although analytical solutions beyond the simplest geometry are rare due to mathematical complexity.

Our main interest in this article is the frequency dependence of the EMI response. By measuring an object's EMI response in a broad frequency band, we attempt to detect and characterize the object's geometry and material composition. We name this potential new technology exploiting the spectral EMI response the *Electromagnetic Induction Spectroscopy (EMIS).*

For low-frequency geophysical applications, the displacement current resulting from the dielectric property may be ignored up to a megahertz and higher. At zero frequency, we observe the induced magnetism from a permeable (i.e., magnetic) object; this is the foundation of the magnetic method. In this sense, the magnetic method is a subset of the EMI method at zero-frequency with the earth's magnetic field as the inducing source.

From numerous EMI surveys that we have conducted using our multifrequency sensors[1,2], we have accumulated ample evidence that a buried metallic object undergoes continuous changes in phase as the transmitter frequency changes. For

Part of the SPIE Conference on Detection and Remediation Technologies for Mines and Minelike Targets III
Orlando, Florida • April 1998
SPIE Vol. 3392 • 0277-786X/98/$10.00

instance, we have commonly noticed that the observed anomalies have opposite polarities at certain frequencies, depending on whether the target is ferrous or nonferrous. It appears that the phase also depends on the target's geometrical shape. These observations are tantalizing in that the EM anomaly measured in a broad band offers an ability to both detect and identify a target.

Certainly, any elementary EM theory makes it obvious that an object must exhibit different responses at different frequencies. All fundamental EM equations involving a time-varying source testify as such. The reason why the subject has not been explored, in our opinion, is due to the lack of *practical* broadband EMI instruments to study the phenomenon. Most commercial EMI sensors (including metal detectors) operate at single frequency or, rarely, at a few discrete frequencies. Because of this spectral limitation, there have been more application interests in the "geometrical sounding" method (an expanding transmitter-receiver array at single frequency) than in the "frequency sounding" method (a fixed transmitter-receiver geometry with varying frequencies). On the research level, however, there have been many experimental works that studied broadband EMI phenomena[3,4,5,6].

The GEM-3 broadband EMI sensor is suitable for high data-density surveys in a short time with minimal logistics[2]. The GEM-3 sensor, weighing about 5 kg, can measure up to 12 data points per second at multiple frequencies between 90 Hz to about 24 kHz, and have a data-logging capacity of about 50,000 points before downloading into a portable computer. Recent experiments indicate that many buried objects manifest different anomaly polarities at different frequencies. Thus, we suspected the possibility of identifying an object based on its frequency response.

To support the experimental observation, we must first establish a firm theoretical basis for the EMIS concept. In this article, we summarize the mathematics necessary for some simple models to study theoretically the EMIS response, followed by field examples.

THEORETICAL CONSIDERATIONS

To explore and understand the EMIS principle, we first consider solid sphere--a simple object that has an analytic solution under a broadband EM illumination. We want to compute the object's response using combinations of electrical conductivity, magnetic permeability, and sensor geometry with respect to the object and frequency.

SPECTRAL RESPONSE OF A CONDUCTIVE AND PERMEABLE SPHERE

In a series of classical papers, Wait[7,8,9,10,11] pioneered in deriving the response of a conductive and permeable sphere suspended in whole space. Others considered more complicated models often involving varying conductivity, layered spherical shells, and conductive host media[12,13]. The models, however, were commonly investigated to understand the response of mineral deposits for mining exploration and, therefore, their solutions have not been applied to the study of small, manmade, highly conductive and permeable objects in a broad spectral domain.

Let us consider the spectral response of a conductive and permeable sphere excited by a dipole magnetic source. Figure 1 shows the geometry of the problem with the following notations:

m_r *or* m_θ: radial or transverse dipole moment,
r_0: radial distance of the dipole transmitter,
a: radius of the sphere, and
(r, θ): the receiver location.

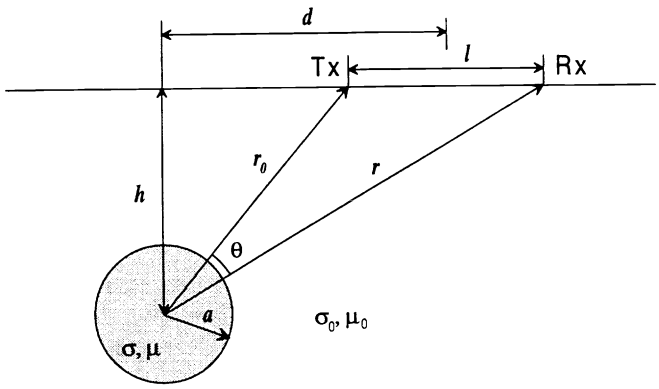

Figure 1. Geometry and notations of a conductive and permeable sphere.

By solving Maxwell's equation with appropriate boundary conditions, one can derive the following spherical harmonics solutions for the secondary magnetic field in the presence of a radial or a transverse magnetic dipole source as depicted in Figure 1. We adopt the expressions and notations used by Grant and West[14], and assume a temporal dependency of $e^{i\omega t}$ for all components.

The radial component of the secondary field due to a radial dipole source is given by:

$$H_{r,r} = -\frac{m_r}{4\pi}\sum_{n=1}^{\infty}(X_n + iY_n)\frac{a^{2n+1}}{(rr_0)^{n+2}}\,n\,(n+1)\,P_n(\cos\theta), \tag{1a}$$

while the transverse component due to a radial dipole source is:

$$H_{r,\theta} = -\frac{m_r}{4\pi}\sum_{n=1}^{\infty}(X_n + iY_n)\frac{a^{2n+1}}{(rr_0)^{n+2}}\,n\,P_n^1(\cos\theta). \tag{1b}$$

P_n is the n-th order Legendre polynomial while P_n^1 is the Associated Legendre polynomial. For a transverse dipole, we assume that it always points toward the receiver dipole (Figure 1), which is common to most fixed-geometry EM sensors. For this case, the radial component of the secondary magnetic field is given by:

$$H_{\theta,r} = \frac{m_\theta}{4\pi}\sum_{n=1}^{\infty}(X_n + iY_n)\frac{a^{2n+1}}{(rr_0)^{n+2}}\,n\,P_n^1(\cos\theta), \tag{1c}$$

while the transverse component due to a transverse dipole is:

$$H_{\theta,\theta} = -\frac{m_\theta}{4\pi}\sum_{n=1}^{\infty}(X_n + iY_n)\frac{a^{2n+1}}{(rr_0)^{n+2}}\left\{n^2 P_n(\cos\theta) - \frac{n}{n+1}\cot\theta\,P_n^1(\cos\theta)\right\}. \tag{1d}$$

The complex expression $(X_n + iY_n)$ in Eqs. (1a) through (1d), called the *response function,* contains all EM properties and the size of the sphere. The remaining terms, all real, are governed only by the relative geometry between the sphere and the source and receiver locations. The real part of the response function, X_n, generates the inphase response and the imaginary part, Y_n, generates the quadrature response of the sphere. For a solid, conductive, and permeable sphere, the response function can be shown as:

$$X_n + iY_n = \frac{\left\{\frac{1}{2} - \eta(n+1)\right\} I_{n+\frac{1}{2}}(ka) + ka \cdot I'_{n+\frac{1}{2}}(ka)}{\left\{\frac{1}{2} + \eta n\right\} I_{n+\frac{1}{2}}(ka) + ka \cdot I'_{n+\frac{1}{2}}(ka)} \quad \text{where } \eta = \mu / \mu_0, \tag{2}$$

in which $k^2 = i\omega\mu\sigma$ and

μ_0: permeability of the host medium,
μ: permeability of the sphere, and
σ: conductivity of the sphere.

$I_{n+1/2}(ka)$ is the modified spherical Bessel function of the first kind at an order $n+1/2$ and has a first derivative $I'_{n+1/2}(ka)$. Lohda and West[13] describe computational difficulties and their remedies associated with Eq. (2) particularly when the order n is high or Θ is very small or very large. In our approach, we computed the ratio I / I' using the continuous fractions representation, which made the higher order computation possible. The *response parameter* (often called the *induction number*) is defined by:

$$\textit{Response Parameter: } \Theta = |ka| = \sqrt{\omega\mu\sigma}\, a. \tag{3}$$

We emphasize that $(X_n + iY_n)$ of Eq. (2) is described completely by (i) the response parameter Θ and (ii) the permeability ratio η and, thus, contains all basic information necessary to predict its behavior under a dipole excitation.

An EM field decays through a conductive medium; the skin depth δ, defined as the distance through which the field decays to e^{-1} (or about 37%) of its original amplitude, is expressed by:

$$\textit{Skin Depth: } \delta = \sqrt{\frac{2}{\omega\mu\sigma}}. \tag{4}$$

Eq. (3) now may be written in terms of the skin depth of the sphere:

$$\textit{Response Parameter: } \Theta = \sqrt{2}\,\frac{a}{\delta}. \tag{5}$$

Figure 2 shows the computed X_n and Y_n (n = 1 to 340) as a function of Θ for the case when the sphere, suspended in free space, is conductive but not permeable (thus $\mu = \mu_0$ or $\eta = 1$). For small Θ (low frequency, resistive limit), both the real (inphase) and imaginary (quadrature) parts are small (thus, little response) but the imaginary part is dominant. For a large Θ (high frequency, conductive limit), the real part is dominant and asymptotically approaches 1. The imaginary part peaks at a particular Θ that is related to the target's physical properties.

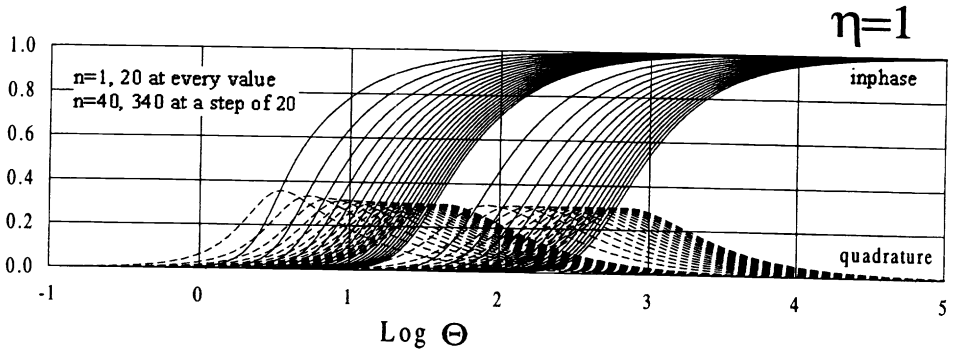

Figure 2. Behavior of X_n and Y_n for an electrically conductive but magnetically nonferrous sphere.

Figure 3 shows another case when the target is permeable, having a permeability ratio η = 500, a representative value for common steels. The quadrature behaves similar to the previous case, while the inphase exhibits large negative values for small Θ. Unlike the conductive sphere of Figure 2, the inphase now is dominant for small Θ. This is the permeability limit at zero frequency, or the DC magnetic response. At a very low frequency, a ferrous sphere is magnetized along the external field lines which, in this case, are generated by a magnetic dipole transmitter. Figure 3 also indicates that the negative inphase changes its sign at a particular Θ for each n and, thereafter, becomes positive as Θ increases. At the crossover, the target becomes invisible in the inphase.

We note in Figures 2 and 3 that both X_n and Y_n change considerably when the Θ changes by a few decades. Therefore, if we can measure the response in a broad range of Θ, we should be able not only to detect the sphere but, based upon the observed response, determine its EM properties and geometry as well.

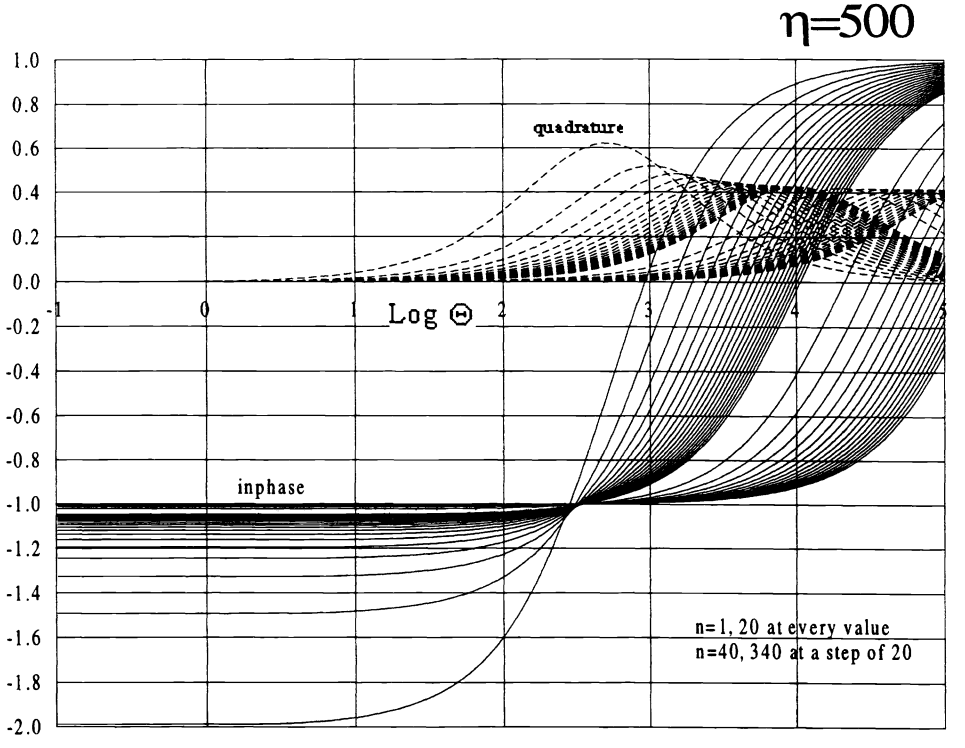

Figure 3. Behavior of X_n and Y_n for an electrically conductive and magnetically permeable sphere.

THEORETICAL EXAMPLES

Figure 4 shows the anomaly (inphase and quadrature) computed for the GEM-3 sensor geometry. The target is a metal sphere having a 15-cm radius and a conductivity of $2 \cdot 10^6$ s/m. The GEM-3 is assumed to be directly above the sphere with the T-R coils in a horizontal plane (i.e., both coils in a vertical-dipole mode). The anomaly is expressed in a unit of parts-per-million (ppm). The frequency axis (x-axis) is a log-frequency unit between 2 (100 Hz) and 5 (100 kHz). The vertical axis, the distance between the sphere center to GEM-3, extends from 0.25 m to 2.5 m. The upper two graphs of Figure 4 show the case when the sphere is conductive but not permeable (η=1). In the lower two graphs, the sphere is both conductive and permeable with a relative permeability of 500. The difference in spectral response between the two spheres is remarkable. We observe from Figure 4 the following features:

- The inphase anomaly of a conductive-permeable sphere changes its sign at a specific frequency (the crossover frequency f_c) that slightly depends on the sensor height. For the conductive-only sphere, in contrast, the f_c is too low to be useful for EMIS. The f_c is rather sensitive to permeability and, therefore, it can be used to determine the content, or possibly the type, of magnetic material of the sphere.

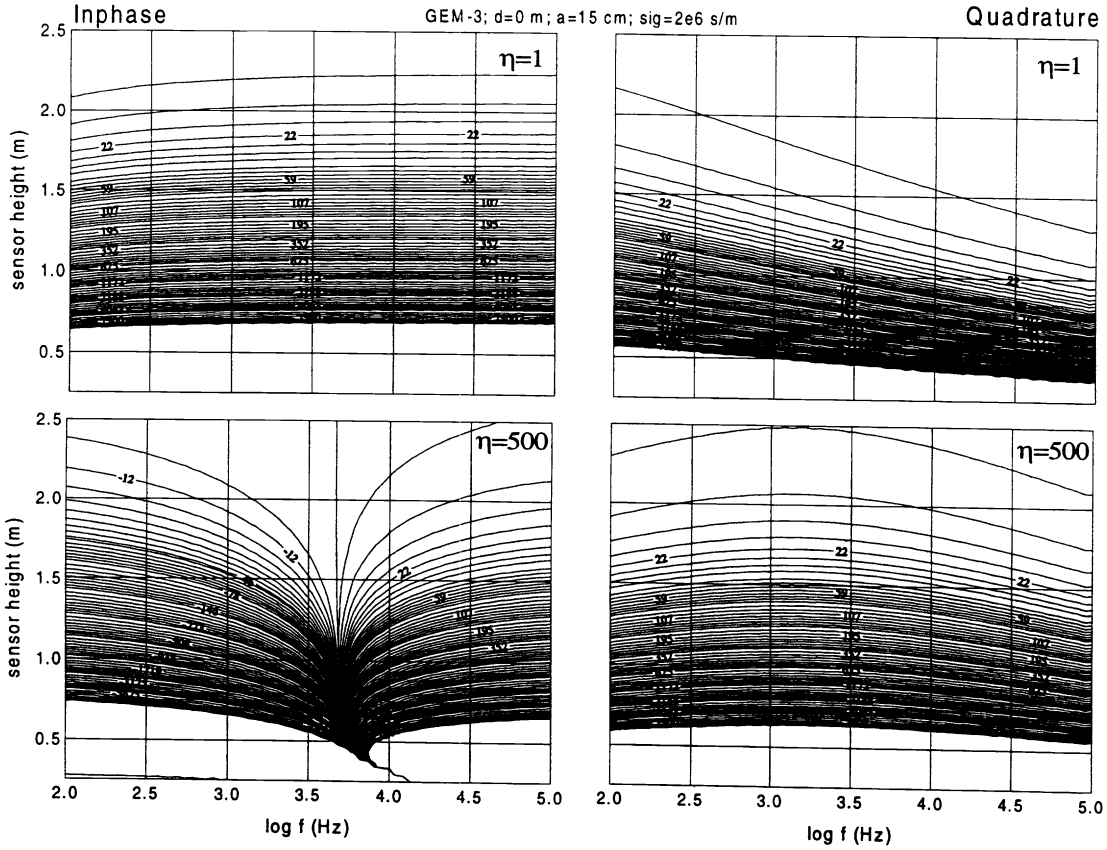

Figure 4. Spectral response (computed for the GEM-3 geometry) of a sphere having a 15-cm radius and a constant conductivity of 2x106s/m. The GEM-3 is placed directly above the sphere. For the upper two graphs, the sphere is only conductive. For the lower two graphs, the sphere is also permeable. See the text for further details.

- Below f_c, the inphase polarity is opposite between the conductive sphere and the conductive-permeable sphere. The anomaly polarity alone can distinguish whether the sphere is made of a magnetic (e.g., iron) or non-magnetic metal (e.g., aluminum).

- At or near f_c, the sphere becomes invisible to the inphase, which stresses the need for measuring both the inphase and quadrature components. It also implies the necessity of broadband measurements to overcome such blind frequency zones.

Further target discrimination may be possible by studying the field decay rate in distance or as a function of frequency. Because a sphere with a particular radius, conductivity, and permeability would generate a specific response diagram (Figure 4 as an example), we can fingerprint, at least theoretically, all available spherical objects of interest for comparative identification. All spectral features discussed here can be extrapolated to an object having an arbitrary shape.

EMPIRACAL RESULTS

In this section, we present the results of one field survey and one controlled experiment. Although the field survey only utilized two frequencies, the results support theory. The controlled experiment consisted of measuring the broadband EMI response (60 frequencies logarithmically distributed over a bandwidth of 270 Hz to 24 kHz) of an assortment of landmines.

SURVEY

Geophex acquired GEM-3 data at two frequencies over a 62-m by 40-m area in Fort Carson, Colorado. The test site was established by the Defense Advanced Research Projects Agency (DARPA) and the Waterways Experiment Station (WES) to acquire high-density data from various geophysical sensors to aid in the detection and discrimination of buried unexploded ordnance and landmines.

Although we acquired GEM-3 data over the entire site, the data shown in Figure 6 are taken from a calibration lanes that contains emplaced aluminum plates and landmines at known locations. The anomaly signs alone clearly indicate the difference between aluminum (non-ferrous) plates and landmines (low-metal ferrous targets) following the theoretical prediction. For instance, both aluminum plates show positive responses for both the inphase and quadrature, as they should according to the theory (only the 4,050 Hz inphase data is shown here). The two shot-puts show strong negative inphase responses and mostly positive quadrature responses at both frequencies as they should based on the EMIS theory.

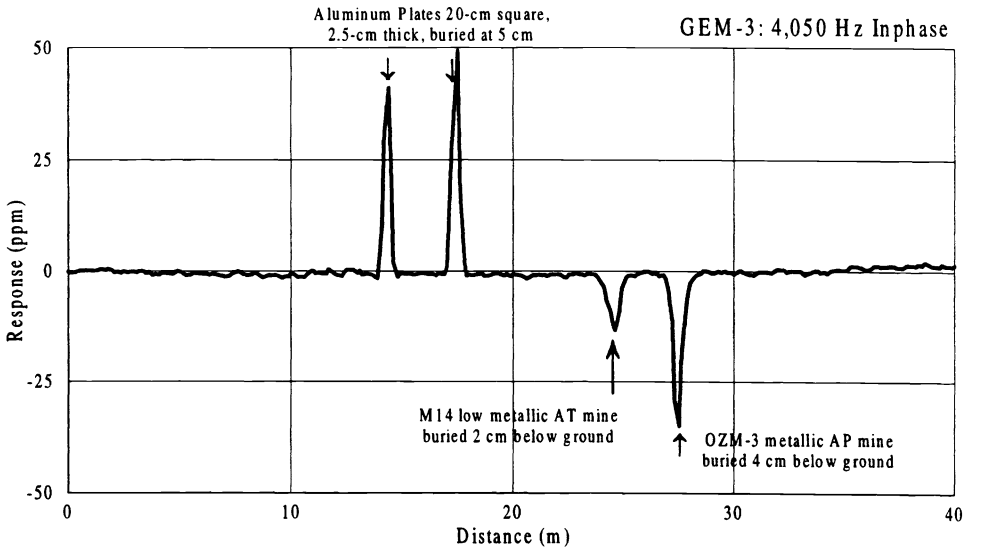

Figure 6. GEM-3 inphase anomaly profile at 4,050 Hz across two aluminum plates and two landmines.

CONTROLLED EXPERIMENT

The controlled experiment consisted of measuring the EMI response of various items using the GEM-3 sensor. For this experiment, the sensor was held rigidly in place on a wooden platform over one meter above the ground. Test objects were place on a plywood table directly under the sensor head. The distance from the object of the sensor could be varied over a wide range. The orientation and horizontal position of the object could be varied as well.

The data collection was controlled by a laptop PC. Multiple broadband sweeps could be collected and downloaded to and ASCII file on the PC in realtime. The frequency range of the data collected was from 270 Hz to 23,970 Hz. A total of 60 frequency steps were taken in logarithmic increments. We recorded data for over 100 calibration targets; including, a 105-mm projectile, 30-mm projectile, solid spheres of various sizes and compositions, plates of various sizes and compositions, Q-coils with a known response, a ferrite rod, clutter items (soda cans, nails, steel banding, etc.), and seven landmines. For all test targets, two consecutive sweeps were taken with and without the object present. This was done to remove the response of the local environment and to eliminate any possible sensor drift. Two identical measurements (i.e., two sets with and without object) were made on each object as a consistency check.

Figure 7 presents the GEM-3 data for the assortment of landmines. The figure shows the measured inphase and quadrature components (left side), a photograph of each mine tested (middle), and a brief description of each mine as stated in a mine handbook.

Although preliminary, the results are very encouraging. The broadband response of particular landmines is distinct and does provide a basis for identification and discrimination. Question: if we are given one of the broadband EMI responses shown in Figure 7, can we identify the associated landmine? These data suggest that it is possible – an encouraging result.

CONCLUSIONS

The purpose of EMIS is to detect and identify hidden metallic objects that can be characterized by their electrical conductivity, magnetic permeability, and geometrical size and shape. To realize fully its potential as a new technology, we need to further develop broadband EMI models and advanced sensor hardware and software.

EMIS technology may be particularly useful for detecting buried landmines and unexploded ordnance. By fully characterizing and identifying an object without excavation, we should be able to reduce significantly the number of false targets. EMIS should be applicable to many other problems where the target identification and recognition (without intrusive search) are important.

ACKNOWLEDGEMENTS

This research was partly funded by an SBIR contract through the U.S. Army Night Vision and Electronic Sensors Directorate in Fort Belvoir, Virginia. Data from Fort Carson, Colorado, was obtained under a contract with the U.S. Army Waterways Experiment Station (WES), Vicksburg, Mississippi, which was, in turn, funded by the Defense Advanced Research Project Office (DARPA).

The GEM-3 sensors are the product of many Geophex scientists and engineers including David Chen, Alex Gladkov, Tom Hall, and Joe Seibert.

REFERENCES

1. Won, I. J., Keiswetter, D. A., Fields, G. R. A., and Sutton, L. C., 1996, GEM-2: a new multifrequency electromagnetic sensor, *Jour. Environmental and Engineering Geophysics*, Vol. 1, No. 2, p. 129-138.
2. Won, I. J., Keiswetter, D. A., Hanson, D. R., Novikova, E., and Hall, T. M., 1997, GEM-3: a monostatic broadband electromagnetic induction sensor, *Jour. Environmental and Engineering Geophysics,* Vol. 2, Issue 1, p. 53-64.
3. Ryu, J., Morrison, H.F., and Ward, S.H., 1972, Electromagnetic depth sounding experiment across Santa Clara Valley, *Geophysics,* v. 37, p. 351-374.
4. Ward, S. H., Pridmore, D. F., Rijo, L., and Glenn, W. E., 1974, Multispectral electromagnetic exploration for sulfides, *Geophysics,* v. 39, p. 662-682.
5. Won, I. J., 1980, A wide-band electromagnetic exploration method: some theoretical and experimental results, *Geophysics,* v. 45, p. 928-940.
6. Won, I. J., 1983, A sweep frequency electromagnetic method, Chapter 2 in *Development of Geophysical Exploration Method - 4,* Editor A.A. Fitch, Elsevier Applied Science Publishers, Ltd., London, p. 39-64.
7. Wait, J. R., 1951, A conducting sphere in a time-varying magnetic field, *Geophysics,* v. 16, p. 666-672.
8. Wait, J. R., 1953, A conducting permeable sphere in the presence of a coil carrying an oscillating current, *Canadian Jour. Physics,* v. 31, p. 670-678.
9. Wait, J. R., 1959, Some solutions for electromagnetic problems involving spheroidal, spherical, and cylindrical bodies, *J. Res. N.B.S.* (Mathematics and Mathematical Physics), v. 64B, p. 15-32.
10. Wait, J. R., 1960, On the electromagnetic response of a conducting sphere to a dipole field, *Geophysics,* v. 25, p. 619-658.
11. Wait, J. R., 1969, Electromagnetic induction in a solid conducting sphere enclosed by a thin conducting spherical shell, *Geophysics,* v. 34, p. 753-759.
12. Fuller, B. D., 1971, Electromagnetic response of a conductive sphere surrounded by a conductive shell, *Geophysics,* v. 36, p. 9-24.
13. Lodha, G. S. and West, G. F., 1976, Practical airborne EM (AEM) interpretation using a sphere model, *Geophysics*, v. 41, p. 1157-1169.
14. Grant, F. S., and West, G. F, 1965, Interpretation Theory in Applied Geophysics, McGraw-Hill Book Co., New York, 584 p.

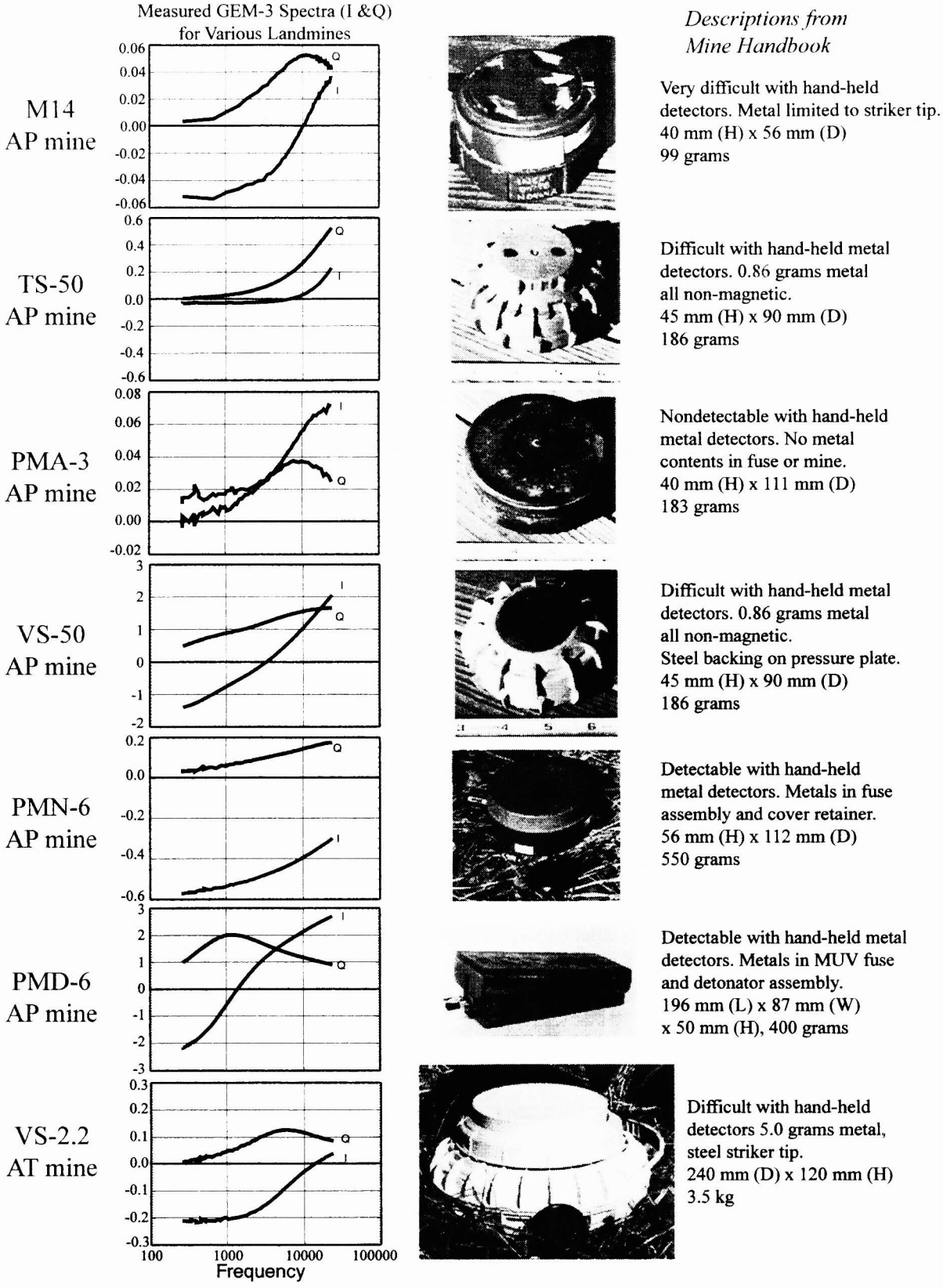

Figure 7. Measured GEM-3 Spectra (Inphase &Quadrature) for Various Landmines.